



Contents lists available at ScienceDirect

Spectrochimica Acta Part A: Molecular and Biomolecular Spectroscopy

journal homepage: www.elsevier.com/locate/saa

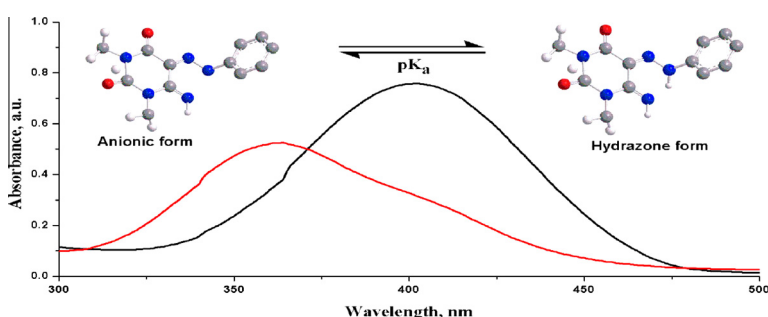
Synthesis, structure and study of azo-hydrazone tautomeric equilibrium of 1,3-dimethyl-5-(arylo)-6-amino-uracil derivatives

Diptanu Debnath^a, Subhadip Roy^a, Bing-Han Li^b, Chia-Her Lin^b, Tarun Kumar Misra^{a,*}^a Department of Chemistry, National Institute of Technology, Agartala 799046, India^b Department of Chemistry, Chung Yuan Christian University, Chung-Li 320, Taiwan

HIGHLIGHTS

- Crystal structure of 1,3-dimethyl-5-phenylazo-6-aminouracil.
- Evidenced azo- and hydrazone forms of azo-derivatives of 6-aminouracil.
- Studied solvent effects on the absorption maxima of the azo-dyes.
- Studied photo-physical property of the azo-dyes.
- Evaluated acid-dissociation constant (pK_a) values of the dyes.

GRAPHICAL ABSTRACT



ARTICLE INFO

Article history:

Received 12 March 2014

Received in revised form 5 December 2014

Accepted 9 December 2014

Available online 29 December 2014

Keywords:

Azo-uracil

Crystal structure

Solvatochromism

Photophysical property

Azo-hydrazone tautomerism

 pK_a

ABSTRACT

Azo dyes, 1,3-dimethyl-5-(arylo)-6-aminouracil (aryl = $-C_6H_5$ (**1**), $-p-CH_3C_6H_4$ (**2**), $-p-ClC_6H_4$ (**3**), $-p-NO_2C_6H_4$ (**4**)) were prepared and characterized by UV-vis, FT-IR, 1H NMR, ^{13}C NMR spectroscopic techniques and single crystal X-ray crystallographic analysis. In the light of spectroscopic analysis it evidences that of the tautomeric forms, the azo-enamine-keto (**A**) form is the predominant form in the solid state whereas in different solvents it is the hydrazone-imine-keto (**B**) form. The study also reveals that the hydrazone-imine-keto (**B**) form exists in an equilibrium mixture with its anionic form in various organic solvents. The solvatochromic and photophysical properties of the dyes in various solvents with different hydrogen bonding parameter were investigated. The dyes exhibit positive solvatochromic property on moving from polar protic to polar aprotic solvents. They are fluorescent active molecules and exhibit high intense fluorescent peak in some solvents like DMSO and DMF. It has been demonstrated that the anionic form of the hydrazone-imine form is responsible for the high intense fluorescent peak. In addition, the acid-base equilibrium in between neutral and anionic form of hydrazone-imine form in buffer solution of varying pH was investigated and evaluated the pK_a values of the dyes by making the use of UV-vis spectroscopic methods. The determined acid dissociation constant (pK_a) values increase according to the sequence of $2 > 1 > 3 > 4$.

© 2014 Elsevier B.V. All rights reserved.

Introduction

Azo compounds, bearing the functional group $R-N=N-R'$, in which R and R' can be either aryl or alkyl, exhibit vivid colors, especially reds, oranges, and yellows resulted from π -electron

delocalization through aromatic moieties. Therefore, they have been used as dyes, known as azo dyes, in textile, food, printing and cosmetic industries [1,2]. The rich chemistry of the azo compounds is associated with several important biological reactions such as protein synthesis, carcinogenesis, azo reduction monoamine oxidase inhibition mutagenic, immune chemical affinity labeling, nitrogen fixation, important medical and industrial uses [3,4]. Recently, in the last two decades, there has been a rapid

* Corresponding author. Tel.: +91 381 2346630; fax: +91 381 2346360.

E-mail address: t_k_misra@yahoo.com (T.K. Misra).

growing interest for their potential applications in miscellaneous areas such as photochromic materials, non-linear optical (NLO) devices, liquid-crystalline displays (LCDs), dye-sensitized solar cells (DSSCs), sensors and indicators as well as biological-medical studies [5–10].

Among the azo dyes, heterocyclic azo dyes attract considerable interest and play an important role in the development of the chemistry of azo compounds. Furthermore, some heterocyclic azo compounds have also found use as ligands to generate a special category of metal azo complexes which are exploited enormously in the manufacture of colorimetric sensors-which lend themselves to cations and anions [11–13]. Of the heterocyclic azo dyes, pyridone and pyrimidine derivatives are relatively recent heterocyclic intermediates for the preparation of aryl-azo dyes [14,15].

Moreover, the applications of azo-dyes are strongly dependent on the photophysical properties of azo-hydrazone tautomerism which has been used to some extent for dye location characterization in surfactant micelles and textile fibers [16,17], photographic systems [18], dyeing protein [19,20], bleaching [21,22], and probe molecules to characterize catalysts [23,24]. Both the tautomers exhibit different optical and physical properties. The hydrazone form that absorbs light at longer wavelengths was therefore found to be rendered higher photoconductivity to dual-layer photoreceptors [18] and it is therefore often commercially preferred. The phenomenon of azo-hydrazone tautomerism correlates the mobility of a labile proton across a molecule through a conjugated system where the proton remains in association with intra-molecular hydrogen bonding between donor-acceptor atoms. Such phenomenon arises when azo dyes contains OH or NHR group conjugated with the azo group.

Study of azo-hydrazone tautomerism mechanism is therefore extremely important and highly demanding for controlling the molecular properties of these systems depending on the polarity and pH of the medium. The study of this property on some dyes has been accomplished and reported [22,25–28] elsewhere. The above observations have drawn our attention and motivated to investigate such interesting property of azo-hydrazone tautomerism on azo-dyes with a backbone of 6-aminouracil derivative. Uracil derivatives, which have pyrimidine-like structure (uracil = pyrimidine-2,4-dione), have an elegance role in heterocyclic chemistry [29]. They have aroused much interest owing to their potential applications in medicine and photobiology [30]. Pyrimidine dyes in some cases prepared from 6-aminouracils have found industrial applications in hypnotic drugs [31], in living cells, in detecting cancer [32] and having pharmacological and biological activities [33]. The detail synthesis of azo derivatives of uracil has been paid attention recently and aryl/hetarylazo derivatives of uracil or 1,3-dimethyl-6-aminouracil have been reported [34–37] by several authors. However, so far no report on the isolation of single crystal X-ray structure analysis of azo-derivatives of 1,3-dimethyl-

6-aminouracil has been reported. The crystal structure of Cu(II), and Rh(III) complex of 1,3-dimethyl-5-(phenylazo)-6-aminouracil had been reported [38,37]. A formation of super-complex of the cationic form of 1,3-dimethyl-5-(phenylazo)-6-aminouracil with AuX_2^- ($X = Cl$ or Br) and its crystal structure had also been reported [39,40]. In this contribution, we report (i) a modified route of synthesis of four azo-derivatives of 1,3-dimethyl-6-aminouracil (Scheme 1); (ii) first time the X-ray crystal structure of 1,3-dimethyl-5-(phenylazo)-6-aminouracil of its azo-tautomeric form which is found stable in the solid state, (iii) the study of solvatochromic property in various organic solvents with different hydrogen bonding parameters and azo-hydrazone tautomeric equilibrium in aqueous solution of varying pH to evaluate the pK_a values, and (iv) the potential photophysical property of the derivatives of 1,3-dimethyl-5-(aryloazo)-6-aminouracil.

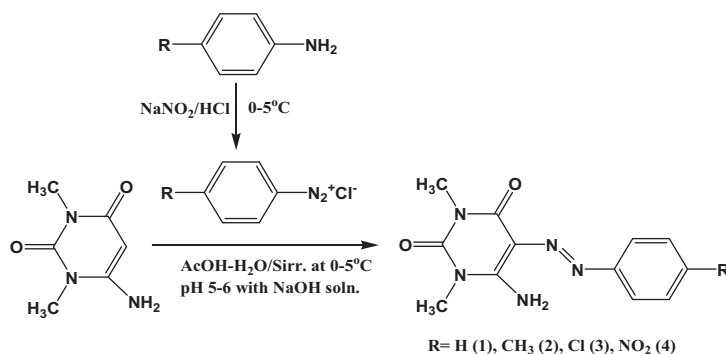
Experimental

Material and instruments

All chemicals were of reagent grade, purchased from Merck, Aldrich, and Himedia and were used without further purification. All solvents were of A. R. grade and used for synthesis and spectroscopic studies. 1,3-Dimethyl-6-aminouracil was prepared following the reported method [41]. For the studies of equilibrium constant double distilled water was used.

Standard Buffer solutions with pH 1.5, 2.0, 3.48, 3.8, 4.39, 4.76, 5.13, 6.04, 9.0, 9.6, 10.0, 10.4, 10.8, and 12.0 were prepared by following the traditional procedure from double distilled water with HCl, NaOH, $Na_2B_4O_7$, $NaHCO_3$, Na_2CO_3 , and KCl. The constant ionic strength of 0.1 M was maintained with KCl solution. In most cases, the pH needed to be adjusted using a pH meter and the drop-wise addition of either 1 M HCl or 1 M NaOH to 1 L of solution. The accurate pH for each buffer solution was measured with a Sytonics digital pH meter 335.

Melting points were determined on a Labtech Digital melting point apparatus with a heating rate of 2 °C/min and not corrected. IR spectra were recorded on a Perkin Elmer; model RX-1 FT-IR spectrophotometer in the region 4000–400 cm^{-1} making KBr pellets of all dyes. 1H NMR and ^{13}C NMR spectra were recorded on a Bruker (AC) 300 MHz and a Bruker DRX-500 MHz FT-NMR spectrometer in $CDCl_3$ as the solvent and TMS the internal standard. The electronic spectra were determined on a Shimadzu UV-vis-1800 spectrophotometer. Quartz cuvettes were used for measurements in solution. Fluorescence spectra of all dyes were recorded in different solvents on a Perkin Elmer spectrofluorometer, model LS55. Excitation and emission slits were set to 10 and 5 nm, respectively. Elemental analyses were made by a Perkin Elmer 2400 series-II analyzer and the results agreed well with the calculated values.



Scheme 1. A general reaction scheme of synthesis of dyes (1–4).

Synthesis of the dyes

All the dyes were prepared following the conventional diazotization process with some modification. As a typical example, aniline (0.651 g, 7.0 mmol) was precipitated out as a salt of aniline hydrochloride and made a solution by adding 5 mL of water. It was then placed in an ice bath and cooled down its temperature to 0–5 °C. An aqueous solution of sodium nitrite (0.484 g, 7.0 mmol in 10 mL of water) was added slowly into the cooled stirred aniline-hydrochloride solution. A light yellow solution, generally called diazotized solution of aniline, formed and was allowed to stir further 30 min at the same temperature. 1,3-Dimethyl-6-aminouracil (1.0 g, 6.46 mmol) was dissolved in hot glacial acetic acid (5 mL) and to make a clear solution 3 mL of distilled water was added. The solution was also then placed in an ice bath to cool it to 0–5 °C. To this solution the diazotized solution was then added slowly with constant stirring for 30 min. A solution of sodium hydroxide (4%) was instilled into the reaction mixture to make the pH ~ 5–6. A bright yellow color precipitation was started to appear. The stirring was continued at r.t. for additional 1 h. The resulting precipitate was filtered, washed with cold water and dried over air oven. The product was recrystallized from hot ethanol and gave brown plate crystals of 1,3-dimethyl-5-(phenylazo)-6-aminouracil.

1,3-dimethyl-5-(phenylazo)-6-aminouracil (**1,3-DM-5-PA-6AU**) (**1**)

Bright yellow crystal, Yield: 78%; M.pt. 258–260 °C; FT-IR (KBr, ν cm^{-1}). 3274 (–NH₂), 1707, 1628 (–C=O), 1523 (–C=C), 1454 (–N=N–), 1357, 1155 (–C–N); ¹H NMR (CDCl₃, δ ppm). 14.12 (br, 1H, –N–NH–), 8.67 (br, 1H, –NH–), 7.72–7.57 (m, 2H, Ar–H), 7.42 (s, 3H, Ar–H), 3.73–3.36 (m, 6H, N–CH₃); ¹³C NMR (125 MHz, CDCl₃): δ (ppm) 27.2 (CH₃), 27.89 (CH₃), 117.27(CH), 127.26 (CH), 129.76 (CH), 144.12 (C), 151.23 (C=O), 153.45 (C=O), 163.33 (C). Anal. Calcd. for C₁₂H₁₃N₅O₂: C, 55.59; H, 5.05; N, 27.01, Found: C, 55.47; H, 4.99; N, 26.97.

1,3-dimethyl-5-(*p*-methylphenylazo)-6-aminouracil (**1,3-DM-5-p-Me-PA-6AU**) (**2**)

Yellow crystal, Yield: 83%; M.pt. 264–262 °C; FT-IR (KBr, ν cm^{-1}). 3265 (–NH₂), 1700, 1622 (–C=O), 1526 (–C=C), 1450 (–N=N–), 1350, 1166 (–C–N); ¹H NMR (CDCl₃, δ ppm). 14.18 (br, 1H, –N–NH–), 8.87 (br, 1H, –NH–), 7.75–7.62 (m, 2H, Ar–H), 7.40 (s, 3H, Ar–H), 3.72–3.34 (m, 6H, N–CH₃); ¹³C NMR (125 MHz, CDCl₃): δ (ppm) 21.2 (CH₃), 27.24 (CH₃), 28.52 (CH₃), 116.27(C), 117.26 (CH), 129.76 (CH), 137.59 (C), 138.46 (C), 149.23 (C=O), 151.45 (C=O), 164.33 (C). Anal. Calcd. for C₁₃H₁₅N₅O₂: C, 57.13; H, 5.53; N, 25.63, Found: C, 57.01; H, 5.48; N, 25.55.

1,3-dimethyl-5-(*p*-chlorophenylazo)-6-aminouracil (**1,3-DM-5-p-Cl-PA-6AU**) (**3**)

Yellow crystal, Yield: 72%; M.pt. 262–261 °C; FT-IR (KBr, ν cm^{-1}). 3289 (–NH₂), 1712, 1628 (–C=O), 1523 (–C=C), 1448 (–N=N–), 1352, 1162 (–C–N); ¹H NMR (CDCl₃, δ ppm). 13.87 (br, 1H, –N–NH–), 9.00 (br, 1H, –NH–), 7.83–7.67 (m, 2H, Ar–H), 7.46 (s, 3H, Ar–H), 3.81–3.46 (m, 6H, N–CH₃); ¹³C NMR (125 MHz, CDCl₃): δ (ppm) 26.94 (CH₃), 28.12 (CH₃), 115.97(C), 118.02 (CH), 129.34 (CH), 131.57 (C), 139.14 (C), 158.41(C=O), 165.35(C=O), 172.39 (C). Anal. Calcd. for C₁₂H₁₂ClN₅O₂: C, 49.07; H, 4.12; N, 23.84, Found: C, 49.02; H, 4.04; N, 23.78.

1,3-dimethyl-5-(*p*-nitrophenylazo)-6-aminouracil (**1,3-DM-5-p-NO₂-PA-6AU**) (**4**)

Yellow crystal, Yield: 64%; M.pt. 288–286 °C; FT-IR (KBr, ν cm^{-1}). 3389, 3256 (–NH₂), 1680, 1612 (–C=O), 1511 (–C=C), 1434 (–N=N–), 1344, 1153 (–C–N); ¹H NMR (CDCl₃, δ ppm). 14.49 (br, 1H, –N–NH–), 9.33 (br, 1H, –NH–), 7.63–7.47 (m, 2H,

Ar–H), 7.36 (s, 3H, Ar–H), 3.80–3.44 (m, 6H, N–CH₃); ¹³C NMR (125 MHz, CDCl₃): δ (ppm) 27.16 (CH₃), 28.17 (CH₃), 114.21 (C), 115.99 (CH), 125.64 (CH), 127.01 (C), 145.22 (C), 163.31(C=O), 165.56 (C=O), 175.35 (C). Anal. Calcd. for C₁₂H₁₂N₆O₄: C, 47.37; H, 3.98; N, 27.62, Found: C, 47.29; H, 3.92; N, 27.54.

X-ray crystallography

The determination of the crystal class, orientation matrix and accurate unit cell parameters of the dye, 1,3-dimethyl-5-(phenylazo)-6-aminouracil (0.45 × 0.38 × 0.32) was performed using a Bruker APEX-II CCD diffractometer with graphite monochromatized Mo-K α (λ = 0.71073 Å) radiation. The crystal was kept at 295(2) K during data collection. The structure was solved using Olex2 structure solution program by following Charge Flipping solution method [42,43]. All the non-hydrogen atoms were refined with anisotropic thermal parameters. All hydrogen atoms were located by geometrical calculation and rode on the parent atom with isotropic thermal parameters (Uiso(H) = 1.2 Ueq(C or N)). The structure was refined with the SHELXL-2013 [44] refinement package using Least Squares minimization. Crystallographic data and the parameters of structure refinement are summarized in Table 1.

Determination of pK_a values by using spectrophotometry

For the determination of acidity constant (pK_a) values of all the investigated dyes, a stock solution (1.0 × 10^{−3} mol/dm³) of known weight of a particular dye was prepared in DMSO solvent. Required volume of dye solution from the stock solution was put into the aqueous buffer solution to make the final concentration in the order of 1 × 10^{−5} mol/dm³ in the desired buffer solution (20:1, v/v aq. buffer/DMSO). After the preparation of a set of solutions in different buffers, the solution mixtures were settled for 30 min. UV–vis absorption spectra of all the dyes were recorded thereafter. The pK_a values of all the investigated dyes were calculated from the obtained spectra following two well-known methods [45]: (1) half-height method [45a] and (2) modified

Table 1
Crystal data of 1,3-dimethyl-5-(phenylazo)-6-aminouracil (**1**).

Empirical formula	C ₁₂ H ₁₃ N ₅ O ₂
Formula weight	259.27
Temperature	295.15 K
Wavelength	0.71073 Å
Crystal system	Monoclinic
Space group	P2 ₁ /c
<i>Unit cell dimensions</i>	
<i>a</i> (Å)	10.4315(11)
<i>b</i> (Å)	8.1867(9)
<i>c</i> (Å)	14.5684(15)
<i>V</i> (Å ³)	1216.5(2)
<i>Z</i>	4
<i>D</i> _{calc} (Mg m ^{−3})	1.416
Absorption coefficient (mm ^{−1})	0.102
<i>F</i> (000)	544
Crystal size	0.45 × 0.38 × 0.32
2 θ range (°)	3.994–56.652
Index ranges	−13 ≤ <i>h</i> ≤ 12, −10 ≤ <i>k</i> ≤ 10, −19 ≤ <i>l</i> ≤ 19
Reflection observed	3022 [<i>R</i> (int) = 0.0575]
Refinement method	Full-matrix least-squares on <i>F</i> ²
Data/restraints/parameters	3022/0/173
Final <i>R</i> indices [<i>I</i> > 2 σ (<i>I</i>)]	<i>R</i> ₁ = 0.0466, <i>wR</i> ₂ = 0.1167
<i>R</i> indices (all data)	<i>R</i> ₁ = 0.1013, <i>wR</i> ₂ = 0.1539
Goodness-of-fit on <i>F</i> ²	0.859
Largest difference peak and hole (e Å ^{−3})	0.20 and −0.17

limiting absorption method [45b] from the absorption-pH relationship. Moreover, it is the Henderson–Hasselbalch Eq. (1) which relates pH and pK_a to the equilibrium concentration of anionic (A^-) and neutral form of an acid (HA).

$$\text{pH} = \text{p}K_a + \log[A^-]/[HA] \quad (1)$$

Results and discussion

Synthesis and structure

The azo derivatives (azo-dyes), 1,3-dimethyl-5-(arylazo)-6-aminouracil (**1–4**) were prepared by following the modified diazo-coupling process. The diazotized aniline derivatives were subjected for coupling with 1,3-dimethyl-6-aminouracil in acetic acid–water solution followed by neutralization with NaOH solution to prepare the desired azo-dyes (**1–4**). The structures of these dyes were established by studying spectroscopic analysis (UV–vis, FTIR, ^1H NMR and ^{13}C NMR), and X-ray crystal structure. The dyes are fluorescent active and thereby they were subject for studying their fluorescent property in solution. The as-synthesized dyes can exist in three tautomeric forms: azo-enamine-keto (HL_{azo} (**A**)), Hydrazone-imine-keto ($\text{HL}_{\text{hydrazo}}$ (**B**)), and azo-imine-enol ($\text{HL}_{\text{azo-enol}}$ (**C**)) as shown in Scheme 2.

IR and ^1H NMR spectral studies

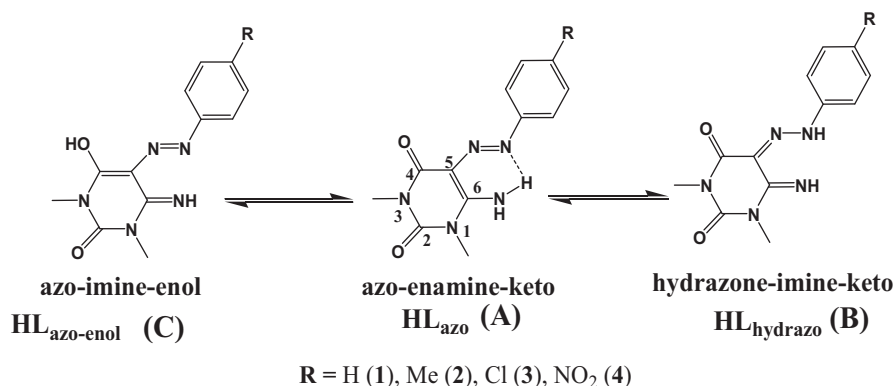
The IR and NMR spectral data for all the isolated azo-dyes (**1–4**) are given in the experimental section. The $\nu(\text{N-H}_{\text{str.}})$ of primary aromatic amines generally appear as bifurcated bands at 3450 and 3390 cm^{-1} [46]. It is somewhat a broad, sharp and strong band at 3274 cm^{-1} for the as-synthesized azo dye (**1**) which is assigned to the N–H stretching frequency of $-\text{NH}_2$ group of the uracil ring [47,48] at the 6-position. The shifting of the band frequency in lower region may be suggested that the $-\text{NH}_2$ group is associated in intra- and inter-molecular hydrogen bonding with the azo-group and keto-group, respectively in the solid state. It has also been evidenced from the crystal structure of the compound (**1**). The aromatic C–H stretching frequency band is overlap with the N–H (6-amino) signal and appeared in the range 3000–3200 cm^{-1} . The sharp intense peaks appeared at 1707 and 1628 cm^{-1} for the dye **1** are due to the carbonyl groups at 2-($^2\text{C}=\text{O}$) and 4-($^4\text{C}=\text{O}$) position of the uracil ring, respectively [47], which rules out the presence of tautomeric form 'C'. The another pair of sharp peaks at 1523 and 1454 cm^{-1} are assigned as $\nu(\text{C}=\text{C})$ and $\nu(\text{N}=\text{N})$, respectively. The appearance of the azo-peak at 1454 cm^{-1} confirms the existence of the tautomeric form

'A' in the solid state. The peaks in the range 1100–1380 cm^{-1} can be attributed to the $\nu(\text{C}-\text{N})$ stretching frequency [48]. The weak bands in the region 943–1058 cm^{-1} are assigned to be ring vibrations. The moderately sharp strong bands at 759 and 692 cm^{-1} are due to the stretching vibrations of N–C=O bonds. The out of plane bending, $\rho(\text{N}-\text{H})$ of N–H bond of the amino group appear at 483 cm^{-1} [45]. A representative spectrum (**1**) is given in Fig. 1. Thus, the IR data reveal that in the solid phase the azo-dyes exist in an azo-enamine-keto (**A**) form.

The ^1H NMR spectral data are also given in the experimental section and a representative spectrum of the dye **1** is shown in Fig. 2. The ^1H NMR spectrum of 1,3-dimethyl-5-(phenylazo)-6-aminouracil (**1**) measured in CDCl_3 at 25 °C shows multiplet signals at δ 3.4–3.7 ppm for six N–CH₃ protons of the uracil ring. The two *ortho*-proton of the aromatic ring appear as multiplet signals at 7.6–7.7 ppm whereas remaining three aromatic ring protons as singlet signal at 7.4 ppm. The tautomeric hydrazone proton (=N–NH–) and imine (=NH) protons appear as broad singlet signal at 14.1 ppm and 8.65–8.67 ppm, respectively. There is no signal found for the –OH proton, ruling out again the presence of the tautomer **C** (Scheme 2). The results are consistent with the reported values [49]. The result may be suggested that the tautomeric form, hydrazone-imine-keto (**B**) (Scheme 2) was predominantly present in the solution. Further evidence was obtained from the study of UV–vis spectra of the dyes in solution.

Crystal structure of **1**

The molecular structure of the molecule, 1,3-dimethyl-5-(phenylazo)-6-aminouracil (**1**) along with the atom numbering scheme is shown in Fig. 3. The selected bond lengths and bond angles are given in Table 2. In uncoordinated azo compounds and hydrazines, the N–N distances are 1.25 [50] and 1.45 Å [51], respectively. In the present azo-dye (**1**), the azo, N(4)–N(5) distance (1.274 Å) is about 0.024 Å longer than the uncoordinated N–N distance, 1.25 Å. The result is comparable with the results (azo–N–N, 1.28–1.30 Å) of two reported crystal structures of this azo-dye where it was found as a protonated form and was isolated with the counter anion AuCl_2^- [52] or AuBr_2^- [53]. In these two reported papers [52,53], authors demonstrated that the protonation of an azo-nitrogen by the extra proton resulted in longer azo bond length. However, our isolated neutral single crystal (**1**), it would be quite apparent from the values of other bond distances (Table 2) that the little longer azo-bond distance may be due to the association of intra-molecular hydrogen bonding rather than protonation. The successive bond lengths involving atoms, N(3), C(7), C(10), N(4), and N(5) are interesting that indicate an existence



Scheme 2. Possible tautomeric forms of 1,3-dimethyl-5-(arylazo)-6-aminouracil: azo-enamine-keto (**A**), hydrazone-imine-keto (**B**), azo-imine-enol (**C**).

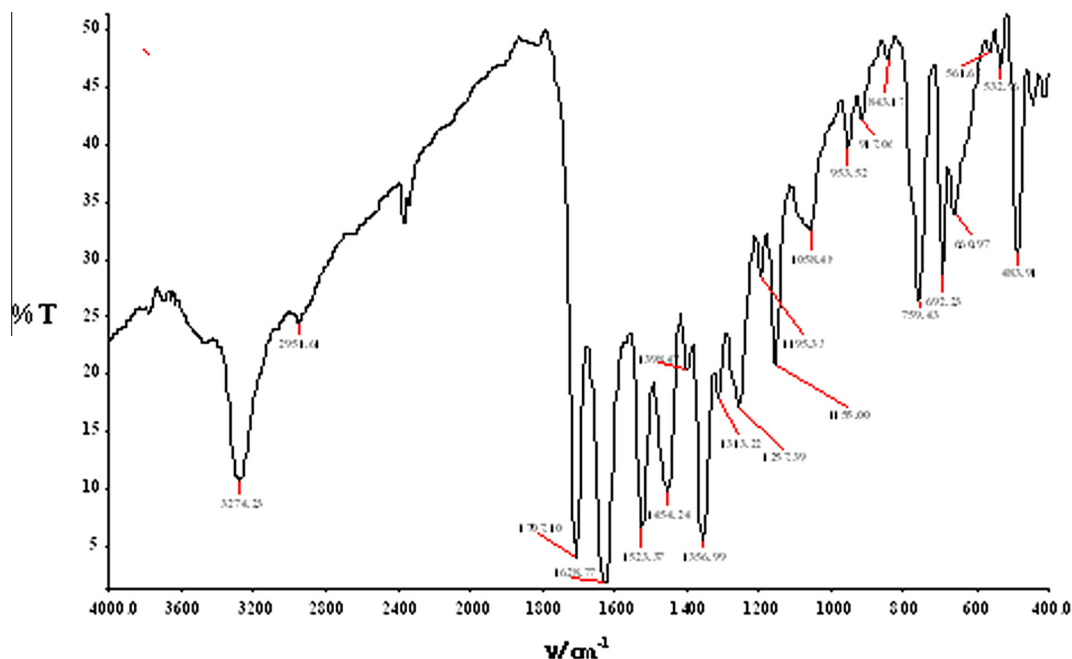
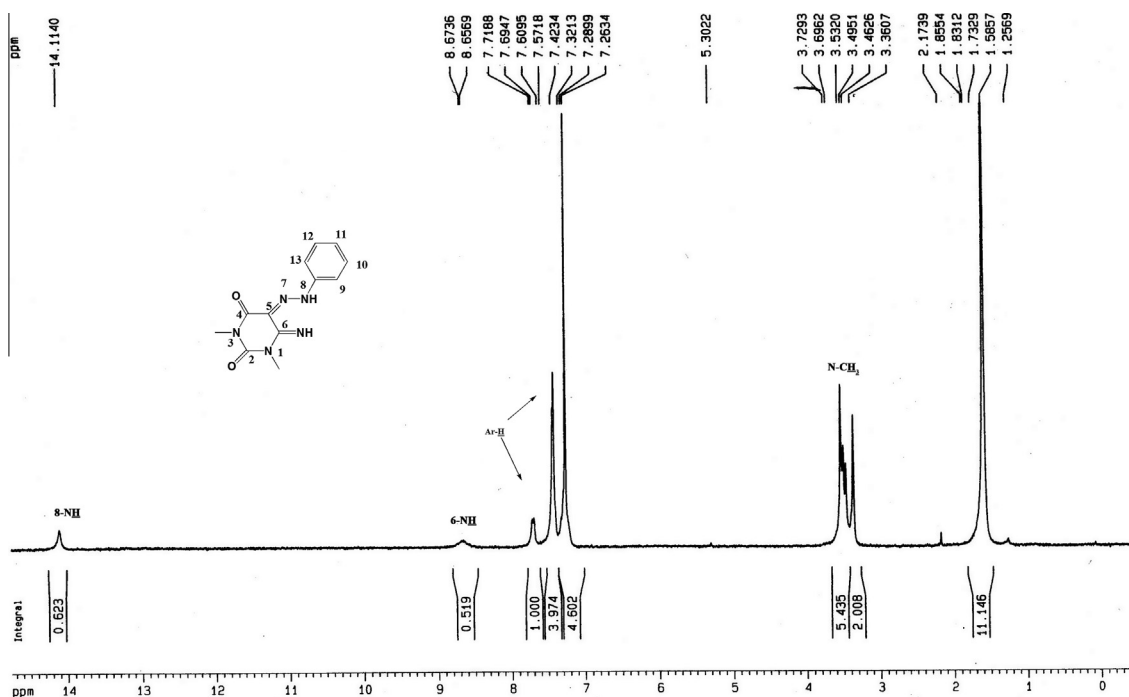


Fig. 1. IR spectrum of the dye 1.

Fig. 2. ^1H NMR spectrum of the dye 1.

of six-membered ring current (resonance hybrids) through these atoms by the association of $\text{N}(3)\text{--H}(3\text{B})\cdots\text{N}(5)$ [$= 1.97 \text{ \AA}$] hydrogen bonding. The $\text{N}_{\text{azo}}\text{--C}$ (phenyl or uracil) bond distances are also indicative that the azo- π -electrons are in pull effect toward the uracil ring. This exo-cyclic $\text{C}(9)\text{--O}(1)$ [$= 1.227(2) \text{ \AA}$] bond distance is slightly longer than that of the other exo-cyclic $\text{C}(8)\text{--O}(2)$ bond [$= 1.212(2) \text{ \AA}$]. It may be the fact that the $\text{O}(1)$ atom is associated with the intermolecular hydrogen bonding with $\text{H}(3\text{B})\text{--N}(3)$. Thus, from the results, it evidences that the dye is in azo-enamine-keto (**A**) form in the solid state. The bond angles within the uracil ring

do not differ much from the expected values. The bond angles of the phenyl ring are also as expected. The molecule is almost planar with a dihedral angle about $10.00(7)^\circ$ between the benzene ring and the uracil ring.

Analysis of the crystal packing of the dye in its unit cell shows the presence of intra- and inter-molecular hydrogen bonding interactions (Fig. 4). The hydrogen bonding parameters are given in Table 3. The $\text{N}(3)$ atom of the 6-aminouracil moiety acts as double two-center hydrogen bond donors. On the other hand, the one nitrogen atom of azo-group, $\text{N}(5)$ act as single two center hydrogen

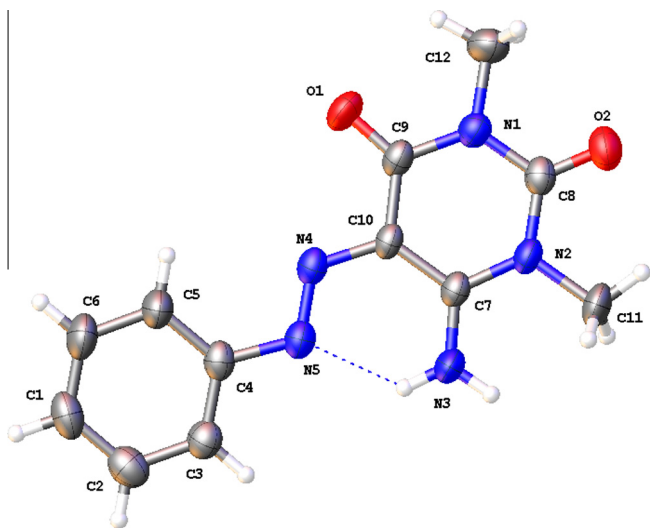


Fig. 3. ORTEP view of the dye **1** with atom labeling scheme and 50% probability thermal ellipsoid.

Table 2
Selected bond lengths (Å) and bond angles (°) of the crystal structure of **1**.

Bond length (Å)			
O(2)–C(8)	1.212(2)	N(4)–C(10)	1.379(2)
N(3)–C(7)	1.314(2)	N(5)–C(4)	1.427(3)
O(1)–C(9)	1.227(2)	C(1)–C(2)	1.367(3)
N(1)–C(8)	1.374(2)	C(1)–C(6)	1.378(4)
N(1)–C(9)	1.399(3)	C(2)–C(3)	1.383(3)
N(1)–C(12)	1.465(3)	C(3)–C(4)	1.381(3)
N(2)–C(7)	1.370(2)	C(4)–C(5)	1.388(3)
N(2)–C(8)	1.388(3)	C(5)–C(6)	1.377(3)
N(2)–C(11)	1.468(2)	C(7)–C(10)	1.409(2)
N(4)–N(5)	1.274(2)	C(9)–C(10)	1.429(3)
Bond angles (°)			
C8–N1–C9	125.05(17)	C6–C5–C4	119.5(2)
C8–N1–C12	116.13(18)	C5–C6–C1	120.7(2)
C9–N1–C12	118.80(17)	N3–C7–N2	118.97(17)
C7–N2–C8	123.01(16)	N3–C7–C10	121.44(18)
C7–N2–C11	120.27(17)	N2–C7–C10	119.59(17)
C8–N2–C11	116.72(17)	O2–C8–N1	122.0(2)
N5–N4–C10	117.70(16)	O2–C8–N2	121.66(19)
N4–N5–C4	114.39(16)	N1–C8–N2	116.32(17)
C2–C1–C6	119.9(2)	O1–C9–N1	118.50(19)
C1–C2–C3	120.0(2)	O1–C9–C10	125.26(19)
C4–C3–C2	120.2(2)	N1–C9–C10	116.23(16)
C3–C4–N5	115.39(18)	N4–C10–C7	126.05(18)
C3–C4–C5	119.59(19)	N4–C10–C9	114.28(16)
C5–C4–N5	125.0(2)	C7–C10–C9	119.67(17)

Table 3
Hydrogen bond distances and angles of the crystal structure of **1**.

D	H	A	d(H···A)	d(D···A)	<(D–H···A)
N(3)	H(3A)	O(1) ⁱ	2.05	2.844(2)	153.0
N(3)	H(3B)	N(5)	1.97	2.605(2)	129.6

Symmetry code: (i) +x, ½ – y, –½ + z.

bond acceptor. The dye units, 1,3-dimethyl-5-(phenylazo)-6-aminouracil, are linked by intermolecular hydrogen bond formation through N(3)–H(3A)···O(1), leading a one-dimensional hydrogen bonded network along b-axis as shown in Fig. 4. Apart from that N(3)–H(3B) forms N(3)–H(3B)···N(5) intra-molecular hydrogen bond with the azo-group.

UV-vis absorption and solvatochromism studies

The electronic absorption spectra of the dyes (**1–4**) were studied over the wavelength range of 200–800 nm, in organic solvents of different hydrogen bonding parameters (δH) [54], viz. non-polar: hexane (Hex) (0.0) and CHCl_3 (5.7); polar-aprotic: CH_2Cl_2 (DCM) (7.1), DMSO (10.2), and DMF (11.3); polar protic: EtOH (19.4), and MeOH (22.3). The aspect of UV-vis spectra is either broad or a peak with a shoulder at longer wavelength as shown in the Fig. 5 (Fig. 5A (**1**); Fig. 5B (**2**); Fig. 5C (**3**); Fig. 5D (**4**)). It can be suggested that the dyes were in an equilibrium mixture of tautomeric forms (**A** and **B**, Scheme 2) or protonated and deprotonated forms of the tautomeric hydrazone form (Scheme 3) in these solvents. Their UV-vis data are given in Table 4. There are two well-defined absorption bands at the wavelength range 260–270 nm and 360–415 nm observed in each spectrum. The former strong band may be assigned to the $\pi \rightarrow \pi^*$ electronic transitions within the aromatic moiety. Sometimes it was difficult to record because of solvent cut-off wavelength in the UV-region. The later absorption band can be attributed to an overlapping band of $n \rightarrow \pi^*$ and $\pi \rightarrow \pi^*$ electronic transitions within the hydrazone/azo form of the dyes [55]. The strong $\pi \rightarrow \pi^*$ transition is generally override the feeble $n \rightarrow \pi^*$ transitions which may or may not be identified from the spectra. The hypsochromic shift of λ_{max} in each case of as-synthesized dyes (**1–4**) was observed with the increase of the value of hydrogen bonding parameters (δH). There was observed some short of deviation in the chlorinated solvents: CHCl_3 and DCM which may be the some sort of interactions occurred between the solvents chlorine atom and the solute dyes. Moreover, the observed λ_{max} shifting (hypsochromic) is more concomitant to hydrogen bonding parameter than to the dipole moment parameter (bathochromic) of the various solvents [1,56]. In the present study, the effect of polar aprotic and polar protic solvents on the

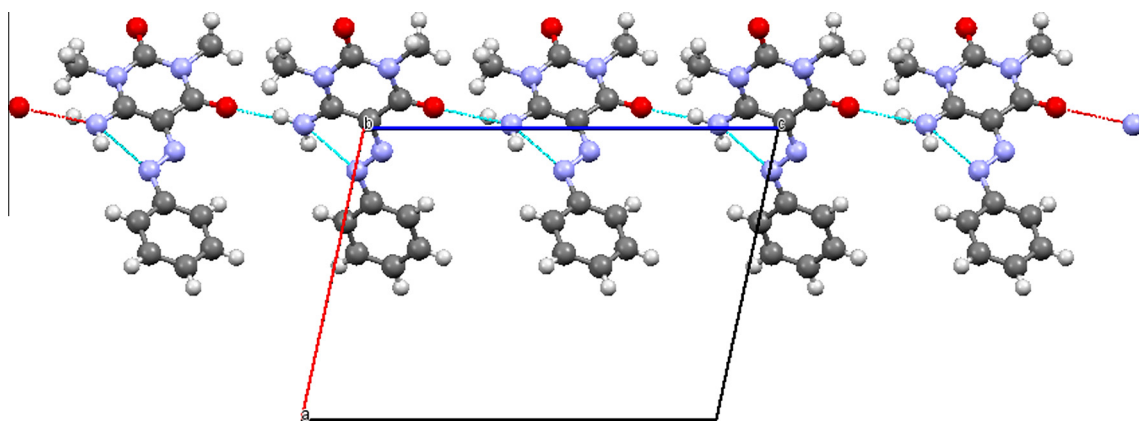


Fig. 4. 1D hydrogen bonding network of the dye **1** along the axis **b**.

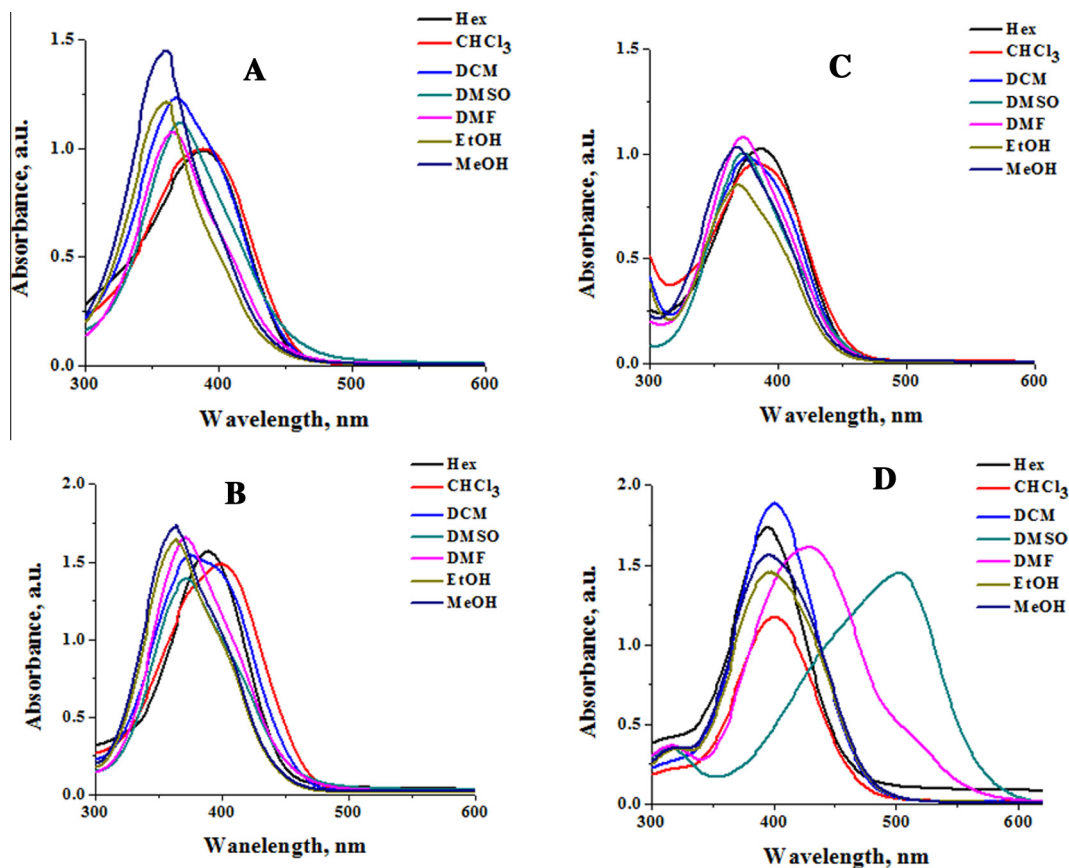
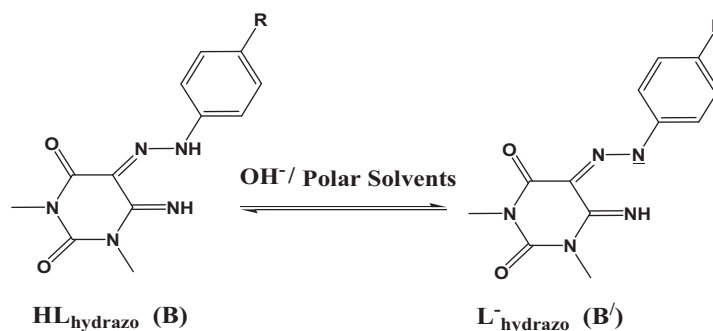


Fig. 5. Solvent effects on electronic absorption spectra of the dyes: 1 (A), 2 (B), 3 (C), and 4 (D).



Scheme 3. Equilibrium between protonated hydrazone-tautomer, HL_{hydrizo} (**B**) and deprotonated hydrazone-anion, L_{hydrizo} (**B'**) forms.

λ_{max} can also be correlated with the dipole moment parameter; the red-shifting of λ_{max} occurs with the increase of their dipole moment parameter. The phenomenon is quite different in case of non-polar solvents. Thus to study the solvent effects considering of hydrogen bonding parameter of the solvents are quite significant. The observed phenomenon is also given a strong indication in the presence of protonated and deprotonated equilibrium rather than azo-hydrazone equilibrium in solution. The solvents having greater hydrogen bonding parameter could stabilize the deprotonated form of hydrazone more effectively than the protonated form. Consequently, blue-shifting of λ_{max} occurs with the increase of δH of the solvents. It can be attributed to the stabilization of the ground state of the deprotonated form through hydrogen bonding interactions. The fact is quite true for the dyes 1–3. Nevertheless, the presence of nitro-substituent at the *para*-position of the benzene ring of the dye 4 destabilize the ground state by bring up

the negative charge onto its head through resonance, as shown in Scheme 4, resulting the reduction of band gap. The λ_{max} of the dye 4 in all solvents is therefore appeared in the red-region compared to the other dyes (1–3).

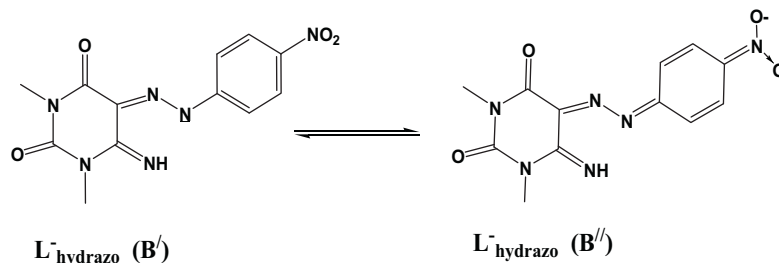
In study of tautomeric equilibrium in acid-base media (later section), the spectrum of each dye exhibited a certain isobestic point which may also be suggested the existence of an equilibrium between hydrazone and hydrazone/azo-anion. The absorption spectra of dyes in hexane and chloroform solvents show single broad absorption bands which have found at the red-region from the far way of their isobestic points. In these two solvents the predominant form of the dyes may be the hydrazone form (**B**) (Scheme 2). The result is also concomitant with the ^1H NMR study. In other solvents the dyes exhibit a strong absorption band with a shoulder at longer wavelength, indicating the separation of $n \rightarrow \pi^*$ transition from the $\pi \rightarrow \pi^*$. The absorption band at shorter

Table 4
Influence of solvent on the electronic absorption properties of azo-dyes (1–4) ($C = 1 \times 10^{-5}$ mol/dm³).

Solvent (δH , H-bonding parameter)	λ_{\max} (nm)			
	1	2	3	4
Hex (0.0)	387	394	383	396
CHCl ₃ (5.7)	390	399	386	401
DCM (7.1)	369, 404 ^{sh}	373, 396 ^{sh}	377, 406 ^{sh}	400
DMSO (10.2)	368, 408 ^{sh}	372, 412 ^{sh}	374, 414 ^{sh}	439 ^{sh} , 502
DMF (11.3)	366, 406 ^{sh}	370, 410 ^{sh}	372, 416 ^{sh}	430, 517 ^{sh}
EtOH (19.4)	361, 402 ^{sh}	364, 410 ^{sh}	370, 407 ^{sh}	397
MeOH (22.3)	360, 401 ^{sh}	363, 410 ^{sh}	368, 409 ^{sh}	397
MeOH + HCl	400	411	400	401
MeOH + NaOH	372, 418 ^{sh}	370, 418 ^{sh}	371	462

wavelength of each dye is ascribed as $\pi \rightarrow \pi^*$ transition. Except in DCM, thus, there is a clear trend of blue-shifting of shorter wavelength band maximum with the increase of hydrogen-bonding parameter of solvents from DMSO (11.3) to MeOH (22.3). The existed equilibrium, in these solvents, may be in between the forms of hydrazone and its anionic form (Scheme 3). The solvent having greater value of hydrogen bonding parameter thus assists deprotonation of the hydrazone form by stabilizing the deprotonated anionic form, with the result that the shorter wavelength band is blue-shifted (hypsochromic shift) accordingly. It is therefore demonstrated that the solvent having high value of δH (3: Hex (0.0), $\lambda_{\max} = 384$ nm–MeOH (22.3), $\lambda_{\max} = 368$ nm) could solvate or stabilize the anionic form of dyes more effectively than the solvent of low δH . The solvatochromic behavior of the as-synthesized azo-dyes is thereby tagged as positive solvatochromism.

To study the effects of acid and base on the absorption maxima of the dyes in solvents like MeOH, 1–2 drop of concentrated HCl or 4 M NaOH solution was added into the MeOH solution of all dyes and noted the change of λ_{\max} . A bathochromic shift ($\Delta\lambda_{\max} = 40$ nm) was observed in each case in presence of acid and practically no shift occurred in presence of base for the dyes. The results show that the dyes could exist in dissociated form i.e. azo- or hydrazone anion in MeOH which is already demonstrated above and the added base had nothing to do on the species present in the solution. The added acid in MeOH, on the other hand, then had protonated the anionic species present in MeOH solution, resulting in the transformation from the anionic species to its protonated hydrazone-tautomeric form (B). Fluorescence results have also yielded the same result. The data in Table 4 are borne out such demonstration. The result seems to be compatible with the hydrazone form rather than the azo form and is consistent with the ¹H NMR data. The existence of anionic form of hydrazone in case of non-N-methylated phenylazo-6-aminouracil was also observed in DMSO and demonstrated by Zeynel and Nermin [56,57].



Scheme 4. Canonical forms of the anionic form of hydrazone tautomer of 1,3-Dimethyl-5-(p-nitrophenylazo)-6-aminouracil (4) where $L_{\text{hydrizo}}(\text{B}')$ -negative charge on the azo-nitrogen and $L_{\text{hydrizo}}(\text{B}'')$ -negative charge on the nitro-group.

Study of fluorescence property and solvent effects

Compounds associated with lowest-energy $\pi \rightarrow \pi^*$ transition exhibit most intense and most useful fluorescence property rather than $n \rightarrow \pi^*$ transition [58]. The lowest-energy electronic transition of our as-synthesized dyes is ascribed as an overlapping strong $\pi \rightarrow \pi^*$ electronic transition along with weak $n \rightarrow \pi^*$ transition of the hydrazone form. The UV-vis study in different solvents as well as in acid-base media of all the dyes (1–4) shows this band in the region of 412–360 nm. Thus the fluorescent property of the dyes was investigated in different solvents. Upon excitation at particular wavelength the dyes (e.g. for 1, $\lambda_{\text{ex}} = 368$ nm in DMSO and $\lambda_{\text{ex}} = 366$ nm in DMF solvents) exhibit strong fluorescent peak (1, $\lambda_{\text{em}} = 437$ nm for DMSO; $\lambda_{\text{em}} = 431$ nm for DMF). The spectra of all the dyes (1–4) showing emissions in different solvents are portrayed in the Fig. 6 (Fig. 6A (1); Fig. 6B (2); Fig. 6C (3); Fig. 6D (4)) and the corresponding data are given in the Table 5. The λ_{em} values obtained from fluorescence spectra are comparable with the obtained electronic absorption data in respect of behavior. However, the most noticeable point is the observed intensity difference of the dyes especially for the dyes 1–3 at their corresponding λ_{em} in different solvents. The observed intensity is in high value in each case in DMSO and DMF whereas in other solvents it is quite low. This observation may be suggested that the fluorescence property of these dyes is due to their anionic forms which are in predominant form in these solvents. Zhang et al. [59] demonstrated that the anionic form of benzotriazole exhibited more strong fluorescence peak than that of its protonated form. DMF and DMSO solvents are the proton acceptor solvents and the existence of the anionic form bearing negative charge is thereby reasonable in these two solvents. In contrast, MeOH and EtOH are proton donor solvents where the negative charge on the anionic form must be in association with hydrogen bonds with these solvent molecules; with the result it is expected to be less fluorescent, i.e. low intense graph. It may also be suggested that the $\pi \rightarrow \pi^*$ electronic transitions of the dyes in these two solvents are no longer remained a lowest-energy transition instead the weaker $n \rightarrow \pi^*$ became the lowest one as it appears as a shoulder peak found in the UV-vis spectra. In other solvents: Hex, DCM, and CHCl₃ the predominant form is the hydrazone form and is suggested to be less fluorescent in these solvents as well. The dye 4 exhibits very low intense fluorescent curve which is justified because of the displacement of the negative charge from the hydrazone head to the nitro-group as shown in the Scheme 4. The results are therefore again evidenced that the predominant form of the dyes in polar aprotic and protic solvents is the anionic form of hydrazone tautomer.

Electronic absorption spectra: study of tautomeric and acid-base equilibria

In addition to the azo-hydrazone equilibrium, the dyes can co-exist in acid-base equilibrium, depending on the pH of the media [60]. The possible acid-base equilibrium of azo-hydrazone

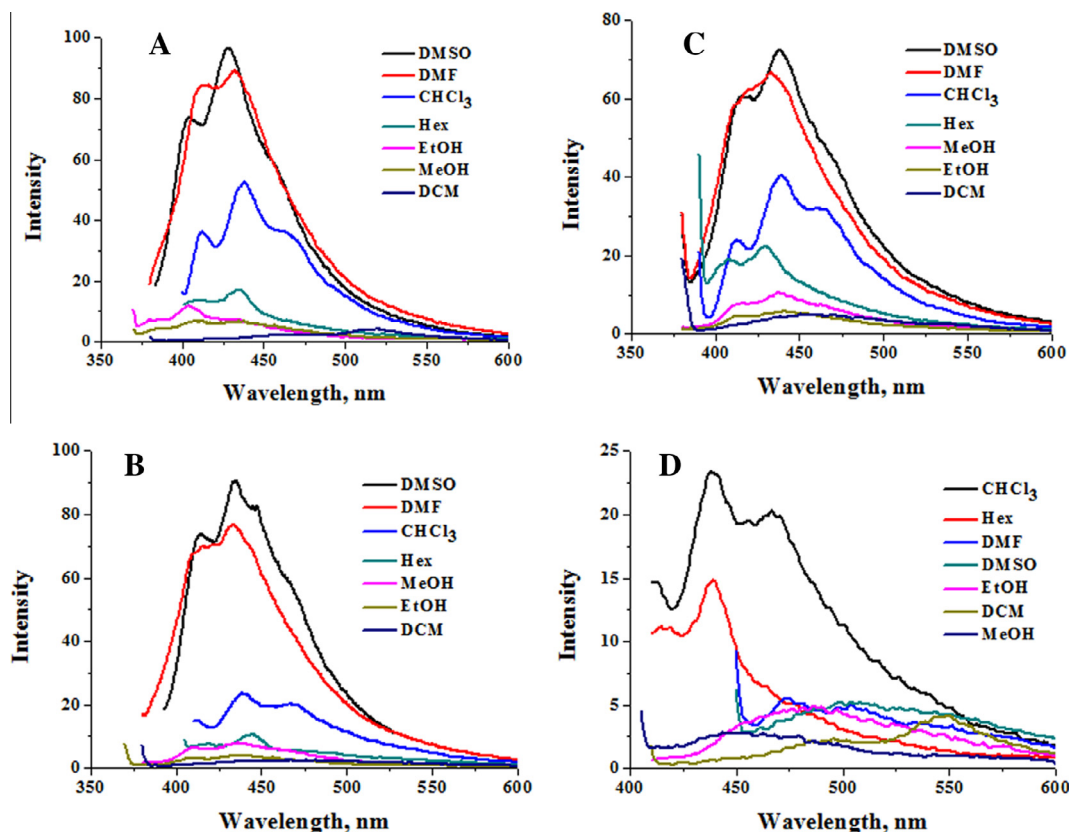
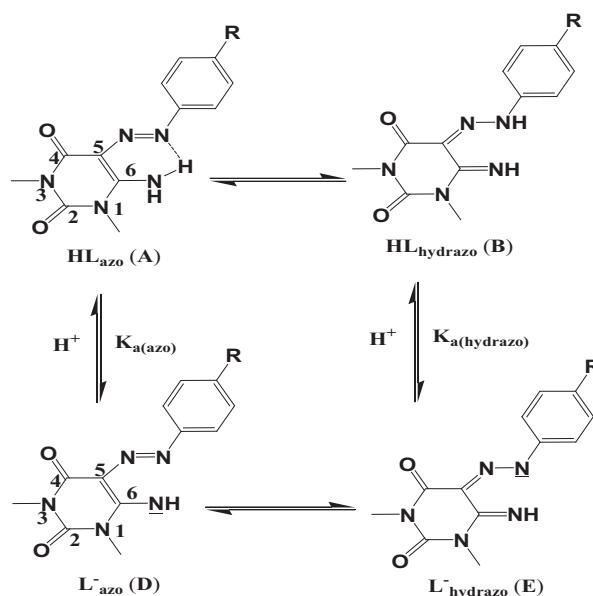


Fig. 6. Fluorescence spectra of the dyes: 1 (A), 2 (B), 3 (C), and 4 (D) in different solvents.

Table 5
Influence of solvent on the emission properties of azo-dyes (1–4), λ_{em} , nm.

Solvent	$\lambda_{ex}, \lambda_{em}/\text{nm}$ (I/a.u.)							
	1		2		3		4	
	λ_{ex}	λ_{em}	λ_{ex}	λ_{em}	λ_{ex}	λ_{em}	λ_{ex}	λ_{em}
Hex	387	433(17)	394	443(11)	383	429(22)	396	439(15)
		440(15)				408(19)		446(12)
CHCl ₃	390	437(53)	399	438(23)	386	438(41)	401	437(55)
		463(36)		466(20)		461(32)		456(38)
DCM	369	434(5)	373	467(2)	377	450(5)	400	549(4)
		459(3)				543(4)		
DMSO	368	437(97)	372	441(77)	374	438(72)	439	498(5)
		414(74)		417(70)		415(61)		532(5)
DMF	366	431(89)	370	433(54)	372	432(67)	430	474(6)
		412(84)		415(41)		424(63)		504(5)
EtOH	361	404(12)	364	437(4)	370	441(6)	397	486(5)
		428(7)		455(3)		436(5)		497(5)
MeOH	360	407(7)	363	436(8)	368	436(11)	397	452(3)
		438(7)		409(6)		432(9)		462(3)

tautomerism of the dyes under investigation is portrayed in Scheme 5. The tautomeric form hydrazone in the equilibrium, forms by the transfer of hydrogen atom from the $-\text{NH}_2$ group to the azo-N atom which is susceptible to form hydrogen bonding with it. Thus, the shifting of a double bond along with a proton transfer leads to the establishment of such tautomerism. In basic media, the formation of azo anion (L_{azo}^- (D)) and hydrazone anion ($\text{L}_{\text{hydrazone}}^-$ (E)) may be suggested to form by the deprotonation from the $-\text{NH}_2$ group of the azo-form (A) and the $-\text{NH}$ group of the hydrazone form (B), respectively. These anionic forms are the indistinguishable resonance hybrids of azo-anion (D) and hydrazone-anion (E) canonical forms.



Scheme 5. Possible acid-base and azo-hydrazone equilibria. The different forms are azo-enamine-keto, HL_{azo} (A), hydrazone-imine-keto, $\text{HL}_{\text{hydrazone}}$ (B), azo-anion, L_{azo}^- (D), hydrazone-anion, $\text{L}_{\text{hydrazone}}^-$ (E), acid dissociation constant for the azo-tautomer ($K_{\text{a(azo)}}$), and acid dissociation constant for the hydrazone-tautomer ($K_{\text{a(hydrazone)}}$).

To study the electronic absorption spectra of these presumed tautomeric and deprotonated forms, the UV–vis absorption spectra of the dyes (1–4) were recorded in the pH range 2.0–10.8 in water and are shown in Fig. 7 (Fig. 7A (1); Fig. 7B (2); Fig. 7C (3); Fig. 7D (4)). The Table 6 is borne out the corresponding λ_{max} data. The

main absorption band which is assigned as an overlapping band of $n \rightarrow \pi^*$ and $\pi \rightarrow \pi^*$ electronic transitions within the hydrazone form [55], is affected most by the change of pH of the media. Moreover, the spectral change (dye **1**) from the pH 2.0 ($\lambda_{\max} = 401$ nm) to pH 10.8 ($\lambda_{\max} = 360$ nm) is noticeable with a well-defined isobestic point at 371 nm. Analogous phenomenon is also observed for the dye **2** as well as **3**. The isobestic point means the existence of an equilibrium between the deprotonated (anionic form: L_{azo}^- or $L_{\text{hydrazone}}^-$) and protonated ($HL_{\text{hydrazone}}$) form of hydrazone. In high acidic media (pH 2.0–3.48), the λ_{\max} of the dyes is affected negligibly, indicating that the hydrazone is the predominant form. As the pH value increases, the intensity of the band decreases initially and further increase of pH leads to the hypsochromic shifts of the λ_{\max} which passes through an isobestic point. In basic media, the absorption band, assigned as $\pi \rightarrow \pi^*$ transition, is suggested to the absorption of the common resonance anion which is the conjugate base of azo and hydrazone tautomers (Scheme 5). Besides, a low intensity shoulder peak appeared at ~ 400 nm in basic medium is assigned as $n \rightarrow \pi^*$ transition which is less sensitive to pH changes to push–pull effects. Unlike dyes **1–3**, for the dye **4** the intensity of the peak at λ_{\max} decreases and becomes broaden without shifting much anyway with the increase of pH. Apart from a shoulder type of peak development occurs in the red region. The results reveal the decrease of concentration of the anionic form of hydrazone ($L_{\text{hydrazone}}^-$ (**B'**)) and the development of the new species $L_{\text{hydrazone}}^-$ (**B''**) due to the strong -I effect of the $-\text{NO}_2$ group as shown in Scheme 4.

Determination of pK_a values of the azo dyes

The acid dissociation constants (pK_a) of the dyes under investigation were determined from their UV–vis spectral behavior in

Table 6
Absorption maxima (λ_{\max}) of the dyes **1–4** at different pH of buffer solutions.

pH	λ_{\max} (nm)			
	1	2	3	4
2.0	402	413	401	404
3.48	401	411	399	404
3.80	399	411	399	403
4.39	400	411	395	402
4.76	367 ^{sh} , 393	367 ^{sh} , 405	387	401
5.13	362, 404 ^{sh}	367, 404 ^{sh}	372, 398 ^{sh}	400
6.04	360, 406 ^{sh}	364, 406 ^{sh}	369, 406 ^{sh}	399, 454 ^{sh}
9.0	360, 406 ^{sh}	363, 406 ^{sh}	364, 408 ^{sh}	400, 454 ^{sh}
9.6	360, 406 ^{sh}	362, 406 ^{sh}	362, 410 ^{sh}	401, 454 ^{sh}
10.0	360, 406 ^{sh}	362, 406 ^{sh}	362, 410 ^{sh}	404, 454 ^{sh}
10.4	361, 406 ^{sh}	362, 406 ^{sh}	362, 412 ^{sh}	408, 454 ^{sh}
10.8	360, 406 ^{sh}	362, 406 ^{sh}	362, 412 ^{sh}	405, 454 ^{sh}
Isobestic point	371	380	374	

Sh: shoulder.

buffer solutions of varying pH 2.0–10.8 at 25 ± 2 °C and are given in Table 7. The concentration of the dyes (**1–4**) in the buffer solution of pH 2.0–10.8 was maintained at 1×10^{-5} mol/dm³. The ionic strength, $\mu = 0.1$ of all the solution was maintained with KCl solution. The dyes (**1–3**, Fig. 7A–C) exhibit two bands with λ_{\max} in region of 360–372 for anionic (L_{azo}^- or $L_{\text{hydrazone}}^-$) and 390–415 nm for molecular species, hydrazone ($HL_{\text{hydrazone}}$) whereas the dye **4** (Fig. 7D) exhibit a single band at ~ 404 nm for both the species. As the pH value of solution increases, the height of the former band for the dyes (**1–3**, Fig. 7A–C) increases simultaneously that of the later decreases; for the dye **4** (Fig. 7D) the band intensity decreases along with a development of a shoulder peak at longer wavelength, as shown in Fig. 7. Each dye except **4** exhibits an isobestic point

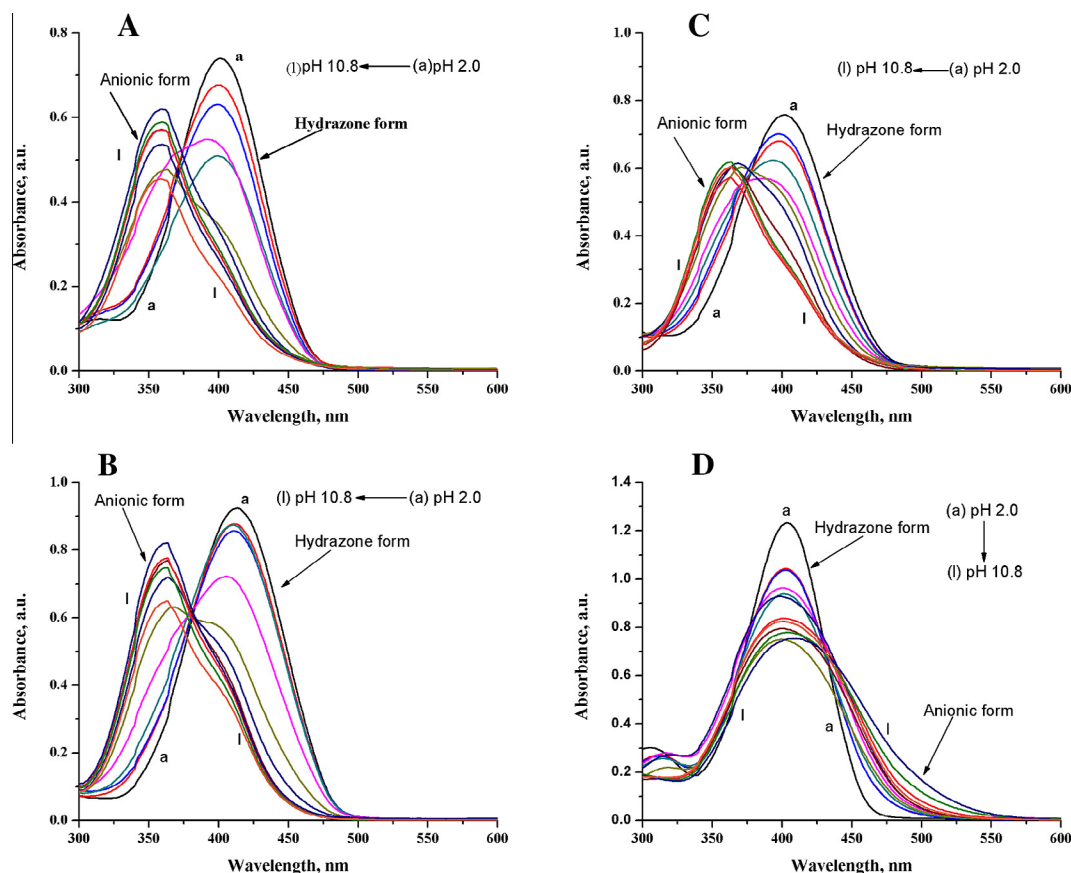
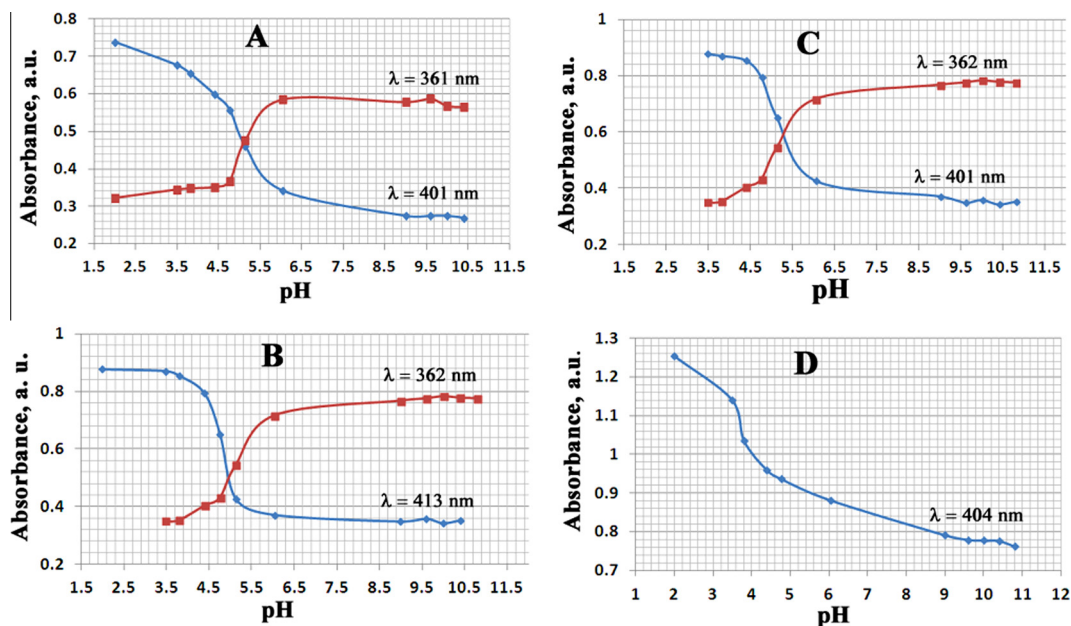


Fig. 7. UV–vis spectra of the dyes: **1** (A), **2** (B), **3** (C), and **4** (D) in the pH range 2–10.8.

Table 7UV-vis spectral data of hydrazone-enamine-keto tautomer of dyes 1–4 and their acid dissociation constants (pK_a).

Dye	λ_{\max} (HL _{hydrazo}), nm	λ_{\max} (L _{hydrazo}), nm	Half height method		Modified limiting method	pK_a (mean)
			pK_a at λ_{HL}	pK_a at λ_L		
1,3-DM-5-PA-6AU (1)	401	361	4.72	4.78	5.28	4.92
1,3-DM-5- <i>p</i> -Me-AA-6-AU (2)	413	362	5.20	5.08	5.15	5.14
1,3-DM-5- <i>p</i> -Cl-AA-6AU (3)	401	362	4.70	4.60	4.66	4.65
1,3-DM-5- <i>p</i> -NO ₂ AA-6-AU (4)	404		3.98		4.29	4.12

**Fig. 8.** Plot of absorbance vs pH: 1 (A), 2 (B), 3 (C), and 4 (D).

which is in the range 371–380 nm, indicating the establishment of equilibrium between the neutral and ionic form. The simplified acid-base and azo-hydrazone equilibrium is shown in Scheme 5. The equilibrium constants can be expressed according to the Eqs. (2)–(4). Where $K_{a(\text{azo})}$ and $K_{a(\text{hydrazo})}$ describe the

$$K_{a(\text{azo})} = \frac{[L_{\text{azo}}^-][H^+]}{[HL_{\text{azo}}]} \quad (2)$$

$$K_{a(\text{hydrazo})} = \frac{[L_{\text{azo}}^-][H^+]}{[HL_{\text{hydrazo}}]} \quad (3)$$

$$K_T = \frac{[HL_{\text{hydrazo}}]}{[HL_{\text{azo}}]} \quad (4)$$

acid-dissociation constant of compounds containing azo-enamine and hydrazone-imine form, respectively and K_T is the tautomeric equilibrium constant. If both the forms, HL_{azo} and HL_{hydrazo} present in the solution quantitatively, the equilibrium constant can be describe with macroscopic pK_a value as expressed in Eq. (5). Where $pK_{a(\text{azo})} = -\log K_{a(\text{azo})}$ and $pK_{a(\text{hydrazo})} = -\log K_{a(\text{hydrazo})}$. The

$$pK_a = \frac{1}{(1 + K_T)} \cdot pK_{a(\text{azo})} + \frac{K_T}{(1 + K_T)} \cdot pK_{a(\text{hydrazo})} \quad (5)$$

study of solution spectra as well as of ¹H NMR spectra reveals that in acidic and neutral solution the most predominant form is the hydrazone-imine form, thereby neglecting the contribution of

$pK_{a(\text{azo})}$ to the Eq. (5) and considering the large value of K_T the Eq. (5) reduces to Eq. (6). The

$$pK_a = pK_{a(\text{hydrazo})} \quad (6)$$

obtained pK_a correspond to pH when the concentration of hydrazone and its anionic form is in equal measured. The pK_a values were determined by making use of two spectrophotometric methods, namely half-height [45a] and the modified limiting absorption [45b] as depicted in Figs. 8 and 9, respectively and both the methods gave concordant results. The constructed absorbance-pH relations at the selected wavelength are sigmoidal curves shaped (Fig. 8A for 1; Fig. 8B for 2; Fig. 8C for 3; Fig. 8D for 4), each comprising a clear inflection, indicating typical dissociation processes (Fig. 8). When plotting the log absorbance ratio vs pH, a straight line is obtained in each case (Fig. 9A for 1; Fig. 9B for 2; Fig. 9C for 3; Fig. 9D for 4); the zero value of the log absorbance ratio indicating corresponding pK_a value (Fig. 9). The pK_a values of all the dyes were evaluated at their corresponding wavelength and these are listed in the Table 7. The values of pK_a fall in the acid region which may be suggested that the dissociable proton must be the hydrazone proton. The determined acid dissociation constants (pK_a) values (Table 7) increases according to the following sequence: $2 > 1 > 3 > 4$. The lower pK_a value of the dye 4 is justified and this is due to the presence of the electron withdrawing group at the *para*-position of the phenyl ring. In contrast, the dye 2 having +R effect of the –Me group at the *para*-position of the phenyl ring possesses comparably higher value.

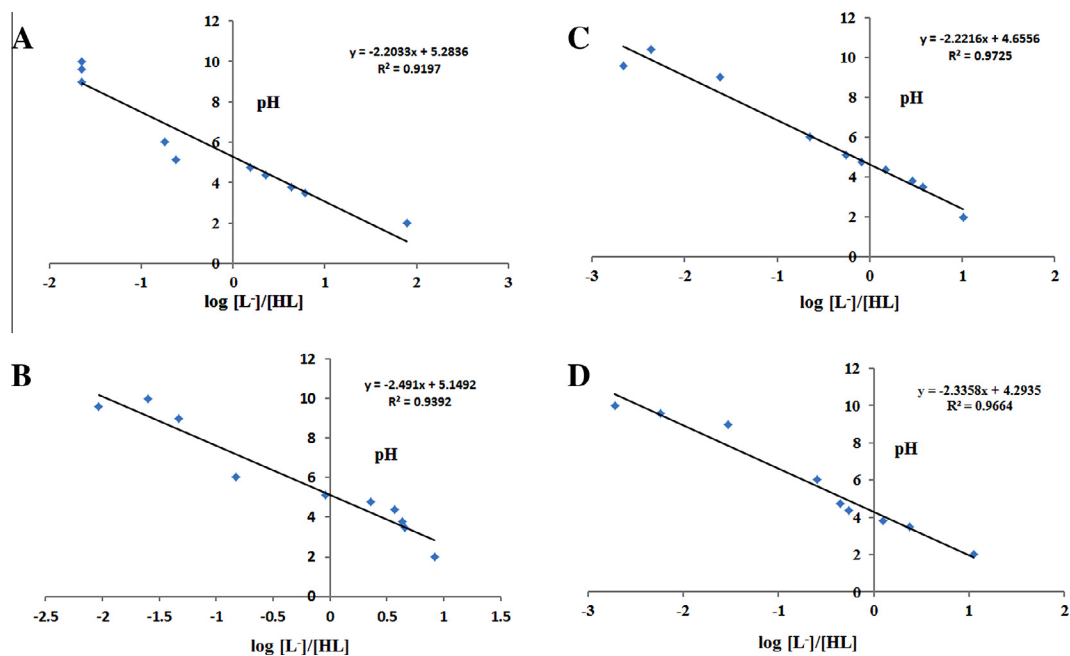


Fig. 9. plot of pH vs $-\log [A - A_b]/(A_a - A)$ where A = absorbance, a = acid and b = basic.

Conclusions

The isolation and characterization of a single crystal structure of an azo dye **1** of **1–4** of the dyes derived from 1,3-dimethyl-6-aminouracil has been executed. The existence of the tautomeric equilibria: azo/hydrazone or hydrazone/its anionic form in different solvents has been studied spectrophotometrically. The azo-enamine-keto form is the predominant form in the solid state. In solution the dyes existed mainly as a mixture of hydrazone-imine-keto and its anionic forms. They show positive solvatochromic property on moving from polar protic to polar aprotic solvents. The dyes exhibit prominent photophysical properties in certain solvents as well. The pK_a values of the dyes indicate that they are easily dissociated to their anionic form not only in the acid medium but also in the solvents of having considerable hydrogen bonding parameter.

Acknowledgement

The authors are very grateful to the Department of Chemistry, NIT, Agartala for providing all kind of supports from all corners. Of the authors D. Debnath is indeed thankful to NIT, Agartala for providing him institutional fellowship. The authors are indebted to Professor C. Sinha for helping in collecting FTIR and 1H NMR spectroscopic data.

References

- [1] M.R. Yazdanbakhsh, M. Abbasnia, M. Sheykhani, L. Ma'mani, *J. Mol. Struct.* 97 (2010) 266.
- [2] N.A. Oranusi, C.J. Ogugbue, *J. Appl. Sci. Environ. Manage.* 9 (2005) 39.
- [3] E. Lohse, *Pharmazie* 41 (1986) 815.
- [4] S. Pati, *The Chemistry of the Hydrazo, Azo and Azoxy Groups*, Part 1, Wiley, New York, 1975.
- [5] E. Ortyl, J. Jaworowska, P.T. Seifi, R. Barille, S. Kucharski, *Soft Mater.* 9 (2011) 335.
- [6] M.M. Raposo, A.C. Fonseca, M.R. Castro, M. Belsley, M.S. Cardoso, L.M. Carvalho, P.J. Coelho, *Dyes Pigm.* 91 (2011) 62.
- [7] V. Chigrinov, H.S. Kwok, H. Takada, H. Takatsu, H. Hasebe, *SID'07 Digest* 45.4 (2007) 1474–1477.
- [8] L. Zhang, J.M. Cole, P.G. Waddell, K.S. Low, X. Liu, *ACS Sustainable Chem. Eng.* 1 (2013) 1440–1452.
- [9] (a) Y. Egawa, R. Gotoh, S. Niina, J. Anzai, *Bioorg. Med. Chem. Lett.* 17 (2007) 3789–3792; (b) Y.Y. Maruo, K. Akaoka, J. Nakamura, *Sens. Actuators B* 143 (2010) 487.
- [10] A.O. Alnajjar, M.E. El-Zaria, *Eur. J. Med. Chem.* 43 (2008) 357–363.
- [11] X. Li, Y. Wu, D. Gu, F. Gan, *Dyes Pigm.* 86 (2010) 182.
- [12] M.A. Diab, A.A. El-Bindary, A.Z. El-Sonbati, O.L. Salem, *J. Mol. Struct.* 1007 (2012) 11–19.
- [13] M.S. Sujamol, C.J. Athira, Y. Sindhu, K. Mohanan, *Spectrochim. Acta A* 75 (2010) 106.
- [14] C. Lubai, C. Xing, G. Kunyu, H. Jiazhen, J. Griffiths, *Dyes Pigm.* 7 (1986) 373.
- [15] N. Ertan, F. Eyduran, *Dyes Pigm.* 27 (1995) 313.
- [16] J. Oakes, S.N. Batchelor, S. Dixon, *Color. Technol.* 121 (2005) 237–244.
- [17] N. Zaghbani, M. Dhahbi, A. Hafiane, *Spectrochim. Acta A* 79 (2011) 1528–1531.
- [18] R. Karpicz, V. Gulbinas, A. Undzenas, *J. Chin. Chem. Soc.* 47 (2000) 589–595.
- [19] M.A. Metwally, E. Abdel-Latif, F.A. Amer, G. Kaupp, *Dyes Pigm.* 60 (2004) 249–264.
- [20] Y.K. Zhao, W.B. Chang, Y.X. Ci, *Talanta* 59 (2003) 477–484.
- [21] N. Menek, E. Eren, S. Topcu, *Dyes Pigm.* 68 (2006) 205–210.
- [22] A. Hassanzadeh, A. Zeini-Isfahani, M.H. Habibi, M.R.A.P. Heravi, M. Abdollahi-Alibeik, *Spectrochim. Acta A* 63 (2006) 247–254.
- [23] S. Pirillo, F.S.G. Einschlag, M.L. Ferreira, E.H. Rueda, *J. Mol. Catal. B* 66 (2010) 63–71.
- [24] S. Pirillo, E.H. Rueda, M.L. Ferreira, *Chem. Eng. J.* 204 (2012) 65–71.
- [25] N.M. Rageh, *Spectrochim. Acta A* 60 (2004) 1917–1924.
- [26] Y.H. Ebead, M.A. Selim, S.A. Ibrahim, *Spectrochim. Acta A* 75 (2010) 760–768.
- [27] A. Ünal, B. Eren, E. Eren, *J. Mol. Struct.* 1049 (2013) 303–309.
- [28] J. Chen, Z. Yin, *Dyes Pigm.* 102 (2014) 94.
- [29] E.B. Tsupak, M.A. Shevchenko, Y.-N. Tkachenko, D.A. Nazarov, *Russ. J. Org. Chem.* 38 (2002) 880–888.
- [30] (a) H. Wamhoff, J. Dzenis, *Adv. Heterocycl. Chem.* 55 (1992) 129; (b) P.G. Ellis, in: E.C. Taylor (Ed.), *The Chemistry of Heterocyclic Dyes*, vol. 47, Wiley Interscience, Chichester, 1987, p. 1.
- [31] W.C. Cutting, *Handbook of Pharmacology*, third ed., Meredith Company, New York, 1967.
- [32] R.M. Izatt, J.H. Christensen, J.H. Rytting, *Chem. Rev.* 72 (1972) 439.
- [33] H. Zeng, Z.P. Lin, A.C. Sartorelli, *Biochem. Pharmacol.* 68 (2004) 911.
- [34] H. Yousefi, A. Yahyazadeh, M.R. Yazdanbakhsh, M. Rassa, E.O. Moradi-Rufchahi, *J. Mol. Struct.* 1015 (2012) 27–32.
- [35] M. Yazdanbakhsh, M. Abbasnia, M. Sheykhani, L. Ma'mani, *J. Mol. Struct.* 977 (2010) 266–273.
- [36] M.S. Masoud, E.A. Khalil, A.M. Ramadan, Y.M. Gohar, A. Swayllam, *Spectrochim. Acta Part A* 67 (2007) 669–677.
- [37] M.I. Arriortua, J.L. Pizarro, J. Ruiz, J.M. Moreno, E. Colacio, *Inorg. Chim. Acta* 231 (1995) 103–107.
- [38] V. Ravichandra, K.K. Chacko, *Inorg. Chim. Acta* 173 (1990) 107–114.
- [39] R. Kivekas, E. Colacio, J. Ruiz, J.D. Lopez-Gonzalez, P. Lion, *Inorg. Chim. Acta* 159 (1989) 103–110.
- [40] J. Suarez-Varela, J.-P. Legros, J. Galy, *Inorg. Chim. Acta* 161 (1989) 199–206.
- [41] F.F. Blicke, H.C. Godt Jr., *J. Am. Chem. Soc.* 76 (1954) 2798–2800.
- [42] O.V. Dolomanov, L.J. Bourhis, R.J. Gildea, J.A.K. Howard, H. Puschmann, OLEX2: a complete structure solution, refinement and analysis program, *J. Appl. Cryst.* 42 (2009) 339–341.

- [43] L.J. Bourhis, O.V. Dolomanov, R.J. Gildea, J.A.K. Howard, H. Puschmann, in preparation (2013).
- [44] G.M. Shelx, Sheldrick, *Acta Cryst. A* 64 (2008) 112–122.
- [45] (a) R.M. Issa, *J. Chem. UAR* 14 (1971) 113;
(b) A.A. Muk, M.B. Pravica, *Anal. Chim. Acta* 45 (1969) 534.
- [46] N.F. Curtis, *J. Chem. Soc. Dalton* (1972) 1357.
- [47] J. Ruiz-Sánchez, E. Colacio-Rodríguez, J.M. Salas-Peregrin, M.A. Romero-Molina, *J. Anal. Appl. Pyrolysis* 9 (1986) 159–170.
- [48] M.S. Masouda, S.A. Abou El-Enein, M.E. Ayad, A.S. Goher, *Spectrochim. Acta Part A* 60 (2004) 77–87.
- [49] E.O. Moradi-e-Rufchahi, A. Ghanadzadeh, *J. Mol. Liq.* 160 (2011) 160–165.
- [50] (a) A. Mostad, C. Romming, *Acta Chem. Scand.* 25 (1971) 3561;
(b) C.H. Chang, R.F. Porter, S.H. Brauer, *J. Am. Chem. Soc.* 92 (1970) 5313;
(c) T. Roy, S.P. Sengupta, *Cryst. Struct. Commun.* 9 (1980) 965.
- [51] Y. Morino, T. Iijima, Y. Murata, *Bull. Chem. Soc. Jpn.* 33 (1960) 46.
- [52] R. Kivekas, E. Colacio, J. Ruiz, J.D. Lopez-Gonzalez, P. Leon, *Inorg. Chim. Acta* 159 (1989) 103–110.
- [53] J. Suarez-Varela, J.-P. Legros, J. Galy, E. Colacio, J. Ruiz, J.D.D. Lopez-Gonzalez, P. Leon, R. Perona, *Inorg. Chim. Acta* 161 (1989) 199–206.
- [54] C. Reichardt, *Solvents and Solvent effects in Organic Chemistry*, Wiley-VCH, New York, 1990.
- [55] C. Toro, A. Thibert, L. de Boni, A.E. Masunov, F.E. Hernandez, *J. Phys. Chem. B* 112 (2008) 929–937.
- [56] Z. Seferoğlu, N. Ertan, *Cent. Eur. J. Chem.* 6 (2008) 81–88.
- [57] Z. Seferoğlu, N. Ertan, *Heteroatom Chem.* 18 (2007) 622.
- [58] D.A. Skoog, E.J. Holler, T.A. Nieman, *Principles of Instrumental Analysis*, fifth ed., Thomson Learning, USA, 1998. p. 360.
- [59] Y.-X. Guo, Q.-F. Zhang, X. Shangguang, G. Zhen, *Spectrochim. Acta Part A Mol. Biomol. Spectrosc.* 101 (2013) 107–111.
- [60] Y.H. Ebead, *Dyes Pigm.* 92 (2011) 705–713.